



Published in final edited form as:

Skin Pharmacol Physiol. 2021 ; 34(4): 214–228. doi:10.1159/000515454.

Micropore closure rates following microneedle application at various anatomical sites in healthy human subjects

Abayomi Tolulope Ogunjimi^a, Christine Lawson^a, Jamie Carr^a, Krishna Kumar Patel^a, Nkanyezi Ferguson^b, Nicole K. Brogden^{a,b}

^aDepartment of Pharmaceutical Sciences and Experimental Therapeutics, University of Iowa College of Pharmacy, Iowa City, IA, United States

^bDepartment of Dermatology, Carver College of Medicine, University of Iowa, Iowa City, IA

Abstract

Introduction: The continuous availability of open micropores is crucial for a successful microneedle (MN) drug delivery strategy. However, micropore lifetime depends on intrinsic skin functional and anatomical characteristics which vary significantly at different anatomical sites.

Objective: This pilot study explored if differences exist in micropore closure timeframes at three anatomical sites – upper arm, volar forearm and abdomen.

Methods: Healthy subjects (n = 35) self-identifying as Asian (n=9), Bi-/multi-racial (n=2), Black (n=9), Latino (n=6) and White (n=9) completed the study. The upper arm, volar forearm and abdomen were treated with MNs; skin impedance and transepidermal water loss (TEWL) were measured at baseline and post-MN to confirm micropore formation. Impedance was measured for 3 days to evaluate micropore lifetime. Measurements of L*, which quantifies skin lightness/darkness, were made using a tristimulus colorimeter. Micropore lifetime was determined by comparing baseline and post-MN impedance measurements, and micropore closure half-life was predicted using mathematical modeling.

Results: Post-MN increase in TEWL and decrease in impedance were significant (p < 0.05), confirming successful micropore formation at all anatomical sites. When data were analyzed according to subject self-identified racial/ethnic groups, mean micropore closure time at the abdomen (63.09 ± 13.13 hr) was longer than the upper arm (60.34 ± 14.69 hr) and volar forearm (58.29 ± 16.76 hr). The predicted micropore closure half-life at anatomical sites was abdomen

*Corresponding author: Nicole K. Brogden, PharmD, PhD, Associate Professor, Division of Pharmaceutics and Translational Therapeutics, Department of Pharmaceutical Sciences and Experimental Therapeutics, The University of Iowa - College of Pharmacy, 180 South Grand Avenue, 552 CPB, Iowa City, IA 52242, Phone: 319-335-8752 | Fax 319-335-9349, nicole-brogden@uiowa.edu.

Author Contributions

NB, KF, CL, and JL contributed to study conceptualization. AO, JC, and CL carried out the study procedures. AO performed all data analysis; all authors contributed to data review and interpretation. AO, KP, and NB wrote and edited the manuscript. All authors reviewed and approved the final manuscript. NB was responsible for acquiring funding for the study.

Statement of Ethics

All studies followed the guidelines set forth by the World Medical Association Declaration of Helsinki.

Approval from The University of Iowa Institutional Review Board was granted prior to enrollment of subjects, and all subjects provided written informed consent prior to participation ([ClinicalTrials.gov](https://clinicaltrials.gov/ct2/show/study/NCT03657277) identifier NCT03657277).

Conflict of Interest Statement

Authors declare no conflict of interest.

(25.86 ± 14.96 hr) \approx upper arm (23.69 ± 13.67 hr) $>$ volar forearm (20.2 ± 11.99 hr). Differences were not statistically significant between groups. Objective categorization by L^* showed that darker skin may be associated with longer micropore closure time at the abdomen site.

Conclusions: Our results suggest that anatomical site of application may not be a source of significant variability in micropore closure time. These findings may help reduce the number of physiological parameters that need to be explicitly considered when developing drug products to support MN-assisted drug delivery strategies.

Keywords

Microneedle; Micropore closure time; Anatomical sites; Transdermal drug delivery

Introduction

Transdermal delivery is a route of administration that presents many advantages, allowing therapeutic delivery of molecules that are susceptible to high first-pass metabolism, or are sensitive to enzymatic and pH-dependent degradation occurring from oral administration. Additionally, transdermal delivery is patient friendly, noninvasive, and provides steady-state concentration of active moieties in the blood for longer durations [1]. Unfortunately, only specific compounds possessing smaller molecular weight, appropriate lipophilic/hydrophilic balance, and low daily dose requirements can effectively cross the stratum corneum (SC) and produce the anticipated systemic response. The SC is the outermost layer of the epidermis, comprised of multiple layers of protein-rich corneocytes arranged in an extracellular lipid matrix. This skin layer effectively limits the diffusion of ions, water, hydrophilic drugs, and macromolecules [2]. In addition, the skin has high inter- and intra-individual variability that may depend on various physiological factors including skin color, age, sex, and anatomical location [3]. Any of these variables, individually or in combination, may influence skin permeability or barrier properties [4]. All commercially available transdermal patches are approved for application only at specific body sites because of the variation in drug absorption that can occur from application to other locations on the body [5, 6].

Numerous physical and chemical enhancement techniques have been developed with the goal of expanding the types of compounds that can be delivered through the skin. Microneedles (MNs) are a noninvasive and painless physical enhancement method that have demonstrated promising translational clinical use. Specifically, skin pretreatment with solid MNs produces transient microchannels (also known as micropores) in the SC without activating sensory nerves in the dermis. This enables efficient passive diffusion pathways for drug molecules of larger molecular weight or hydrophilic nature, and also avoids limitations of conventional transdermal therapy including low flux and slow onset of action [7].

The success of the MN pretreatment approach relies on effective formation of micropores. Subsequently, the length of time that a drug can be delivered through those micropores depends on the micropore healing rate or closure time. Micropore closure time is known to be affected by physiological variables such as age [8] and skin type [9], but how it is affected by anatomical treatment site remains largely unexplored. Such consideration could be

fundamental for determining the specific dose, dosing frequency, and ideal site for drug application with MN pretreatment to attain the desired therapeutic response over a specified timeframe. Though direct comparisons of skin response to MN application at various anatomical sites are lacking, it is reasonable to hypothesize that this variable may affect the rate at which micropores heal, thereby also affecting the extent and rate of drug absorption at that site.

There are almost no data comparing variation in skin characteristics and response to MN treatments at different anatomical sites. Therefore, this pilot human study was focused on specifically exploring skin barrier properties and skin recovery at various anatomical locations in healthy human subjects after disruption of the skin barrier with MN application. We further aimed to study if there are additional differences in micropore closure based on race/ethnicity or skin color. This study is the first of its kind to simultaneously characterize the skin barrier properties and microneedling response on micropore closure time at different anatomical locations.

Materials and Methods

Microneedle arrays

In-line stainless steel MN arrays were purchased from Tech Etch (Plymouth, MA), and needles were manually manipulated to be perpendicular to the base. Each array contained 50 needles of 800 μm length. Arrays were sterilized prior to use and affixed to AR7717 adhesive backing (Adhesives Research, Glen Rock, PA) to make an adhesive micropatch that was used during MN insertion. The purpose of the adhesive backing is to provide a more consistent and reproducible MN insertion by holding the array in close contact with the skin throughout the application. Occlusive patches were pre-assembled using Scotchpak 1109 SPAK 1.34 MIL heat-sealable polyester film (3M, St. Paul, MN), a moisture impermeable backing. A silicone rubber ring (FDA White Buna 60 durometer; Ilene Industries Inc., Shelbyville, TN) was fixed to the impermeable backing using double-sided tape (3M, St. Paul, MN). The final occlusive coverings were sterilized prior to use.

Human subjects and enrollment

All studies followed the guidelines set forth by the Declaration of Helsinki. Approval from The University of Iowa Institutional Review Board was granted prior to enrollment of subjects, and all subjects provided written informed consent prior to participation ([ClinicalTrials.gov](https://clinicaltrials.gov/ct2/show/study/NCT03657277) identifier [NCT03657277](https://clinicaltrials.gov/ct2/show/study/NCT03657277)). This study enrolled healthy, non-obese individuals aged 18-50 years. Subjects were asked to self-identify their racial/ethnic group(s) according to the following categories: Asian, Black, Latino, Native American, White, Bi-/multi-racial, or other. Subjects meeting the following criteria were excluded from the study: BMI >29.9 , history of inflammatory dermatologic diseases, current inflammation or irritation at any skin site used in the study, impaired or altered immune function, use of prescription or over-the-counter medications (oral contraceptives and multivitamins were allowed), or allergy to materials used in the study. Subjects with impaired ability to understand and provide consent were also excluded from enrollment.

Measurements of epidermal properties

Hydration, transepidermal water loss (TEWL), electrical impedance, and skin color were measured at all sites at baseline. Hydration was measured using a CM 825 Corneometer probe with an MPA 6 adapter system and MPA CTplus software (Courage + Khazaka Electronic, Köln, Germany). The probe was gently cleaned using a KimWipe® prior to each measurement. The probe was placed gently against the skin for approximately 5 seconds until a measurement was recorded in arbitrary units in the software. TEWL measurements were made using an open chamber evaporimeter with the associated software (cyberDERM Inc, Broomall, PA). The probe was held gently in contact with the skin for ~40-60 seconds, or until the measurement stabilized. Electrical impedance measurements were taken using an EIM-105 Prep-check Electrode Impedance Meter (General Devices, Ridgefield, NJ) with a 200 k Ω parallel resistor (IET Labs Inc., Westbury, NY) and measurement and reference electrodes connected via lead wires to the impedance meter. Measurements were taken in triplicate for 30 seconds at each site, using a new Series 800 Ag/AgCl wet gel measurement electrode (S&W Healthcare Corp, Brooksville, FL) at each site. A new reference electrode (Superior Silver Electrode with PermaGel; Tyco Healthcare Uni-patch, Wabasha, MN) was used at each visit. Skin color was recorded using unitless L* (light-dark) values obtained from a tristimulus colorimeter (ChromaMeter CR-400; Konica, Minolta, Japan). The device was calibrated prior to use at each study visit using the associated white calibration plate. To make measurements, the instrument head was placed in contact with the skin surface for ~5 seconds while the color reflectance was measured.

Microneedle application and micropore formation

Each MN treatment site was cleaned with an alcohol swab and allowed to dry. A sterilized MN array with adhesive backing was then applied to the site using gentle and consistent pressure (applied by the researcher's thumb) for ten seconds. The array was removed, rotated 45 degrees, and applied a second time to form 100 micropores at the site. This MN application process is similar to previous reports [2, 8–10].

Study design

Informed consent and all study visits were conducted at the University of Iowa Clinical Research Unit. Following consent, subjects participated in a total of four visits: one for baseline measurements and MN application, and three follow-up visits. At each visit subjects were asked to sit quietly in the study room for thirty minutes in order for their skin to acclimate to ambient conditions. During the first visit, five sites were identified at each of three anatomical locations (15 sites total): upper arm, volar forearm, and abdomen (Figure 1). The five sites at each anatomical location received the following treatment: MN treatment to form micropores (n=3), occlusion with patch but no MN treatment (occlusion control, n=1), and no MN treatment or occlusive patch (negative control, n=1). Site configurations were consistent across all subjects. All MN-treated sites and the occlusion control sites were covered with an occlusive patch immediately following measurements. All patches were covered with Tegaderm® (3M, St. Paul, MN) to secure the patch in place and protect from water.

The overall study design is seen in Figure 2. Hydration, TEWL, electrical impedance, and skin color were measured at all sites at baseline. The measurements were always made in that order to prevent influence of gel impedance electrodes on hydration-sensitive measurements. Following MN application, TEWL and impedance measurements were immediately re-measured (always in that order) to confirm micropore formation. Occlusive patches were applied to the relevant sites and subjects left the clinic for the day. Subjects returned to the clinic for follow-up in 24-hour increments for the next three days. At each visit the occlusive coverings were removed and impedance was re-measured at each site. New occlusive patches and Tegaderm® were applied, except on the final study day. All measurements were conducted at one anatomical location before moving to the next location. To minimize the time that treatment sites were exposed to air, once an occlusive patch had been removed all measurements were made at that site and fresh patches were applied before moving on to the next site. Follow-up was conducted by phone or email within three to four days of the final visit to assess for residual redness and irritation at the treatment sites.

Data Analysis

Baseline skin parameters and epidermal micropore formation—Mean baseline TEWL, impedance, skin color, and hydration at each anatomical site were calculated and compared using paired t-tests. The % increase in TEWL and % decrease in impedance from pre- to post-MN application for each site (at each anatomical location) was calculated from mean TEWL and impedance values for each site. A statistically significant difference between pre- vs. post-MN TEWL and impedance measurements (determined via ANOVA) confirmed adequate micropore formation. Any site that did not demonstrate a statistically significant difference in TEWL or impedance measurements after MN treatment was not included in the analysis.

Calculation of micropore closure time—Impedance measurements at each site were used to determine micropore closure time. The mean of three impedance measurements was calculated for each site on the first study day and all subsequent study days. Individual measurements that differed by 125% from other measurements at the same site were considered to be outliers and excluded from the analysis, in accordance with previous studies [8]. The impedance measurement setup is made up of three independent, parallel pathways for electrical current. The overall measurement (Z_{total}) is composed of the resistor box (Z_{box}), intact skin (Z_{skin}), and micropores (Z_{pores}). The Z_{total} , Z_{box} , and Z_{skin} are known, and thus micropore impedance can be calculated as shown in Equation 1 [10].

$$Z_{total} = \frac{1}{\frac{1}{Z_{box}} + \frac{1}{Z_{skin}} + \frac{1}{Z_{pores}}} \quad (1)$$

Z_{skin} was derived from the occluded control sites on all days except baseline. This was done because the control sites were under the same occluded conditions as the MN-treated sites, accounting for the effect that occlusion and hydration may have had on the measurements.

Mean impedance was further converted to admittance, Y , which is the inverse of impedance. This transformation provides two main advantages. First, admittance follow the same trend as TEWL in which intact skin baseline values are low, but significantly increase when the skin barrier is compromised. This can be used to monitor micropore lifetime because as micropores close the impedance will increase towards its baseline (and therefore, admittance will decrease towards its baseline). This makes data easier to interpret in relation to TEWL, which is one of the most widely recognized parameters to assess skin barrier function. Second, by transforming the data in this way, general pharmacokinetic equations can be applied to the data analysis. This provides an opportunity to calculate more precise micropore closure time in terms of closure half-life.

To determine micropore closure time, the admittance of MN-treated sites was compared to that of occluded non-MN sites at each time point using Student's t -tests. Micropores were determined to be closed when there was no statistically significant difference between the admittance of the MN-treated sites and occluded non-MN sites at a given timepoint (study day). Each subject served as their own control.

Modeling of micropore closure kinetics—The determination of micropore closure time through the statistical comparison between MN-treated sites and occluded non-MN sites described above only gives a simplistic and general idea about the time by which micropores are closed. However, to precisely determine a predictable micropore closure time that will be more useful in clinical settings, a strategy was devised to calculate the micropore closure half-life ($t_{1/2}$). Admittance was normalized to the highest post-MN admittance and the contributions from the occluded non-MN site were subtracted to cancel out the effect of the hydration status of the site. Thereafter, normalized admittance values were logarithmically transformed and plotted against time (hr). The normalized admittance data were used to derive a micropore closure half-life for each subject at each anatomical location according to Equation 2 (a and b are derived parameters), similar to previous studies [8–10].

$$t_{1/2} = \frac{-b \pm \sqrt{b^2 - 4a \ln 2}}{2a} \quad (2)$$

Statistical analysis—One-Way ANOVA was performed to compare TEWL and impedance values pre- and post-MN at each anatomical site. Student's t -tests were performed to compare admittance between MN-treated and occluded non-MN sites at each anatomical location to determine micropore closure time. To evaluate differences in TEWL, impedance, hydration, and micropore closure time between anatomical sites, a paired t -test was performed, $p < 0.05$ was considered statistically significant. GraphPad Prism Software (GraphPad Software, San Diego, CA) was used for all statistical analyses.

Results

Subject demographics

A total of 35 healthy subjects participated in this pilot study (12 males, 23 females) with a mean \pm SD age of 24.9 ± 7.1 years and BMI of 22.8 ± 3.3 . According to self-identified

racial/ethnic background, the demographics of the study population were Asian (n = 9), Black (n = 9), Latino (n = 6), White (n = 9), and Bi-/multi-racial (n = 2).

Baseline epidermal properties

A summary of baseline skin properties is shown in Table 1. Mean baseline TEWL across all subjects was significantly higher on the upper arm vs. abdomen (6.36 ± 2.27 vs. 5.45 ± 1.82 $\text{g/m}^2\cdot\text{hr}$, respectively), $p < 0.05$. There were no significant differences in baseline TEWL between volar forearm (5.98 ± 2.68 $\text{g/m}^2\cdot\text{hr}$) vs. abdomen or upper arm. When data were compared between anatomical sites within each self-identified racial group, baseline TEWL was significantly higher in upper arm vs. abdomen for the Asian (6.92 ± 1.52 vs. 5.68 ± 1.83 $\text{g/m}^2\cdot\text{hr}$), White (6.98 ± 2.67 vs. 5.64 ± 2.16 $\text{g/m}^2\cdot\text{hr}$) and Latino (7.56 ± 2.64 vs. 5.77 ± 2.38 $\text{g/m}^2\cdot\text{h}$) groups, $p < 0.05$. No significant difference in baseline TEWL was observed between any anatomical sites in the Black or Bi-/multi-racial groups.

Mean baseline impedance across all subjects was significantly higher at the abdomen (76.48 ± 28.01 $\text{k}\Omega$) vs. upper arm (65.55 ± 22.17 $\text{k}\Omega$), $p < 0.05$. In like manner, baseline impedance was significantly higher on the volar forearm (72.11 ± 22.56 $\text{k}\Omega$) vs. upper arm. There was no significant difference in baseline impedance between the volar forearm vs. abdomen. Within groups (when classified according to self-identified race), no significant differences in baseline impedance were observed between most anatomical sites of all the racial/ethnic groups. However, baseline impedance was significantly higher at the abdomen (83.55 ± 36.35 $\text{k}\Omega$) vs. upper arm (58.87 ± 28.83 $\text{k}\Omega$) in the Latino group and significantly higher in the volar forearm (85.86 ± 19.99 $\text{k}\Omega$) vs. upper arm (78.78 ± 16.41 $\text{k}\Omega$) in the Black group. When mean baseline impedance at anatomical sites was compared between self-identified ethnic groups, no significant difference was observed between any of the groups.

The unitless measurements of baseline skin hydration were significantly higher on the volar forearm vs. abdomen (28.88 ± 8.3 and 23.24 ± 8.5 , respectively) and higher on the upper arm (28.02 ± 8.94) vs. abdomen across all subjects regardless of race/ethnicity, $p < 0.05$. There was no significant difference in baseline skin hydration between the upper arm and volar forearm across all subjects. Within self-identified racial/ethnic groups, baseline hydration was significantly higher in the upper arm and volar forearm vs. the abdomen (23.90 ± 6.42 and 24.36 ± 4.36 vs. 18.59 ± 5.95 , respectively) in the Asian group. Baseline hydration was significantly higher in the upper arm vs. abdomen (35.08 ± 7.75 and 27.98 ± 5.92 , respectively) in the Black group. Baseline hydration was significantly higher in the volar forearm vs. abdomen (29.60 ± 9.90 and 23.52 ± 8.77 , respectively) in the White group, while it was also significantly higher in the upper arm and volar forearm vs. abdomen (24.14 ± 4.39 and 28.76 ± 8.59 vs. 18.03 ± 5.51 , respectively) in the Latino group.

Micropore formation

TEWL overall significantly increased from baseline to post-MN at all anatomical locations, confirming formation of micropores in the skin (Figure 3A), $p < 0.05$. The % increase in TEWL over baseline was $243.96 \pm 126.33\%$, $264.46 \pm 151.20\%$, and $225.47 \pm 137.67\%$ at the volar forearm, upper arm, and abdomen respectively. The significant increase in TEWL from baseline to post-MN was also observed within each racial/ethnic group investigated in

this study. Table 1 shows a summary of measured TEWL and % change after MN application at each anatomical site within each group.

In a complementary fashion to the TEWL measurements, mean impedance values decreased significantly pre- to post-MN at all anatomical sites (Figure 3B). The % decrease in impedance from baseline was $74.46 \pm 7.91\%$, $69.35 \pm 14.17\%$, and $64.60 \pm 13.71\%$ at the volar forearm, upper arm, and abdomen respectively. The significant decrease in impedance from baseline to post-MN was also observed within each racial/ethnic group.

No significant difference in % increase or decrease in TEWL or impedance, respectively, was observed from baseline to post-MN between anatomical sites and between racial/ethnic groups. This further confirmed an effective MN application procedure and successful micropore formation at all anatomical sites across all racial/ethnic groups investigated.

Micropore closure time

Micropore closure time was determined by a simple analysis in which the micropores were deemed to be “closed” when there was no statistical difference between the MN-treated site and the occluded control site at that anatomical location. Because of the study design and the way these data were collected, micropore closure time for each site could only be determined in 24 hr increments. The overall micropore closure time was then calculated by finding the mean of the micropore closure times across all of the subjects. Figure 4 shows the mean and frequency distribution of observed micropore closure time at the different anatomical sites. Mean micropore closure time at the abdomen (63.09 ± 13.13 hr) was higher than the upper arm (60.34 ± 14.69 hr) and volar forearm (58.29 ± 16.76 hr), though the differences were not statistically significant between any of the sites (paired *t*-test, $p > 0.05$). However, more subjects had a micropore closure time greater than 72 hr at the abdomen ($n=12$) than the upper arm ($n=7$) and volar forearm ($n=8$). Micropore closure time at the various anatomical sites was not significantly different between any of the racial/ethnic groups ($p > 0.05$).

Micropore closure half-life

In order to calculate a micropore closure half-life, impedance values were transformed to admittance and normalized to the highest post-MN admittance at each anatomical site (as described above). The normalized data were logarithmically transformed and fitted to a non-linear second-order polynomial model (Figure 5) to accommodate variability in admittance observed at each anatomical site. Subject profiles that fit the model considerably well with R^2 values > 0.8 were used to estimate micropore closure times; this corresponded to 22, 27, and 21 subject profiles from the abdomen, upper arm and volar forearm, respectively. The remaining profiles at each anatomical site could not be fitted to the model. The ranking of micropore closure half-life for the anatomical sites was abdomen (25.86 ± 14.96 hr) \approx upper arm (23.69 ± 13.67 hr) $>$ volar forearm (20.2 ± 11.99 hr). Although the predicted closure half-life was longer in the abdomen than in the upper arm and volar forearm, there were no statistically significant differences between anatomical sites. However, the micropore closure half-lives appear to loosely correlate with the micropore closure time based on simple statistical analysis, which was overall higher at the abdomen and more subjects had

micropore closure time beyond 72 hr. Using basic pharmacokinetic principles, the window of 3 – 5 half-lives may be used to describe a timeframe during which approximately 87.5 to 97% of micropores would have closed, depicting a time at which drug diffusion through the micropores would likely cease in a pharmacokinetic study. The micropore closure windows of 3 – 5 half-lives were 73.2 – 121.9 hr, 71.1 – 118.4 hr, and 60.6 – 101.0 hr for abdomen, upper arm, and volar forearm, respectively. The mean observed micropore closure times from statistical analysis at the abdomen (63.09 ± 13.13 hr), upper arm (60.34 ± 14.69 hr) and volar forearm (58.29 ± 16.76 hr) overlapped with the predicted 3 – 5 half-lives for each anatomical site investigated.

Discussion

In MN-assisted transdermal delivery, micropore closure time is an important factor that can limit the success and effectiveness of the delivery strategy if the micropores close prematurely and truncate the drug delivery window [2, 8]. Literature has suggested high inter-site variation in SC thickness and barrier functions in the same individual, signifying different physiological and permeability behavior of skin at various anatomical sites including the forehead, cheek, legs, and forearm [11–14]. Skin characteristics that are related to epidermal barrier function have also been shown to differ when measured at various sites on the body [3, 13, 14, 16], and this variability may affect absorption of drugs. Rougier *et al* studied the influence of anatomic sites on skin transportation of benzoic acid and hydrocortisone. They detected that total permeation varied as follows: forehead > abdomen > thigh > chest > arm > back [15]. These differences may also play vital roles in skin recovery rate across different anatomical sites of the body and may influence micropore closure time at these anatomical sites. In support of this hypothesis, some studies have demonstrated that physiologic and demographic factors such as age, race, and ethnicity may affect micropore closure time [8, 9]. In this pilot study we set out to study how differences in anatomical site of MN application may influence micropore closure time. The long-term goal is to use this information to make rational decisions on the anatomical site that will produce an optimal drug delivery window after MN application. Here we demonstrated in a small group of representative subjects that there are not significant differences in micropore closure time between three sites on the body. This suggests that micropore closure may not directly contribute to variability in drug absorption through MN-treated skin at various anatomical locations.

Baseline epidermal properties

We measured TEWL and impedance in this study as a semi-quantitative method for determining micropore formation in the skin. TEWL is a basic parameter that can be used to measure the degree of skin barrier functionality by quantifying the amount of water that is lost through the skin under non-sweating conditions [17]. Variability in TEWL values at different anatomical sites (including some of the sites investigated in the current work) have been reported in previous studies and these variations have been attributed to the structure of epidermis and horny layer at these anatomical sites [18–20]. A report from the standardization group of the European Society of Contact Dermatitis on guidelines for TEWL measurement which summarized TEWL measurements at different anatomical sites

from several studies ranked TEWL as forearm = upper arm = abdomen [12]. Most of these studies showed lower but statistically insignificant TEWL value at the abdomen vs. forearm and upper arm [12, 20]. In our study, although TEWL values across all subjects and within the self-identified Asian, White, and Latino groups were significantly higher in the upper arm vs. abdomen, no significant difference in TEWL values was observed between any sites. Our findings of no significant differences in overall baseline TEWL between anatomical locations is also in agreement with the study of Mohammed *et al* which found no significant difference in TEWL values of the mid-ventral forearm and the abdomen of healthy adult subjects [21]. Although statistically higher TEWL values were associated with upper arm vs. abdomen in the self-identified Asian, White, and Latino groups in the current study, this may not be clinically relevant and is unlikely to influence the success of micropore creation when a MN application procedure is correctly performed [9].

Impedance measurements provide physiological information that can be used as a complementary method to TEWL to assess skin barrier functionality [22]. Impedance measures the response of a skin area to an externally applied electrical current [23], correlating barrier function with change in the resistance to movement of electrical current posed by the SC [2]. It is less sensitive to the hydration status of the skin and can easily measure small changes in electrical resistance of hydrated skin, including at sites where micropores have been created [2]. Many studies have reported significant differences in skin impedance measured at various anatomical locations [24, 25] and attributed these observations to differences in skin thickness, hydration level, and activity of sweat glands [25]. The results in our study showed that baseline skin impedance at the abdomen was significantly higher than at the upper arm across all subjects, and within the Latino and Black self-identified racial/ethnic groups. This higher impedance at the abdomen may be due to the lower skin hydration observed at the abdomen when compared to the upper arm and volar forearm, as studies have shown that increased skin hydration may lead to increased skin permeability and consequently a decrease in skin membrane electrical resistance [26–28].

Skin hydration is important for maintaining healthy skin by supporting optimum physical and mechanical skin properties [29, 30]. In our study, skin hydration was significantly lower at the abdomen vs. upper arm and volar forearm across all subjects, and also within racial/ethnic groups. This result is in agreement with other studies which showed that skin water content is lower at the abdomen when compared to the forearm and upper arm [31, 32]. Several studies have reported a direct relationship between reduced skin hydration and slower wound healing [33, 34]; this may be relevant also in the context of MNs because the newly created micropores could be considered “micro wounds” in the skin that need to heal. In fact, Kelchen *et al* reported longer micropore closure time after MN application in older human subjects [8] whose skin may be associated with reduced hydration [35, 36]. This suggests that baseline skin hydration may have some influence on the barrier functionality of the skin, which may then affect micropore closure. In addition, in our own previous work where we demonstrated the influence of skin color on micropore closure time, we also showed a relationship between low baseline skin hydration, higher skin impedance, and longer micropore closure time [9].

Micropore formation and closure time

The MN applications were well tolerated, and no irritation or pigmentation changes were observed from the MN insertion. This is especially important because darker skin tones are at a higher risk for pigment changes (either hypo- or hyper-pigmentation) and any methods of drug delivery through the skin should avoid inducing these events if possible [37]. TEWL and impedance measurements were used in this study as highly sensitive qualitative and semi-quantitative surrogate measurements of SC barrier functions. These techniques are widely employed to confirm micropore formation and closure in the SC because increased TEWL and decreased impedance both indicate an attenuated skin barrier [8, 9]. Pre- and post-MN TEWL measurements were used to confirm creation of micropores (and thus, a successful MN application procedure) in the current study, and impedance measurements were used as a complimentary technique to further ascertain creation of micropores. TEWL measurements are normally low at baseline but increase in response to skin barrier disruption such as MN application, while baseline impedance in intact skin is high but decreases when the skin barrier is disrupted like in MN application [8–10]. In our current study there was a significant increase overall in TEWL and decrease in impedance from baseline to post-MN application, confirming the successful formation of micropores at all anatomical sites and agreeing with previous studies [8, 9]. Although differences in baseline TEWL and impedance were observed between some anatomical sites across all subjects and within racial/ethnic groups, no significant difference in % change in TEWL or impedance was observed between any of the anatomical sites. This suggests that the MN application procedure was successful at each of the anatomical sites studied and that baseline TEWL or impedance likely does not influence the outcome of a correctly performed MN application procedure (as may have been expected). These findings may be important when MN products are in the development and manufacturing stage because according to these preliminary results, anatomical location of MN insertion may not be a factor that needs to be considered for successful application of the MNs themselves.

Immediately after the successful creation of micropores by MN application to the skin, the most important factor that can limit the diffusion of drug from a formulation patch placed over the MN-treated site into the systemic circulation is the length of time the micropores stay open [2, 8]. Disrupted skin restores its barrier to prevent infection or entry of harmful substances, but with micropores there is a balance that needs to be attained such that a drug can be delivered for long enough to achieve the desired therapeutic effect and maintain it for a relevant length of time [38]. Earlier studies in human subjects reported micropore lifetimes ranging from 15 minutes [39] to a few hours [40] when the micropores are not under occlusion. Some contemporary advanced studies describing the effect of MN geometry (length, radius or shape) [41–43] and occlusion [38, 44, 45] suggested these as crucial parameters which can significantly influence micropore closure and therapeutic efficacy. However, a clinical evaluation on the volar forearm revealed that MN length and use of occlusion over the micropores could dramatically prolong the pore recovery (up to 48-72 hours) by creating larger channels, enhancing hydration, and retarding the synthesis of lamellar body and lipids essential for repair [46, 47]. Other studies also showed that innate skin barrier functions associated with age and racial background can influence the micropore closure time after MN application [8, 9].

Direct comparisons of skin response to MN application at various anatomical sites and across different racial and ethnic groups are lacking, though it is reasonable to expect that anatomical site differences may affect the rate at which micropores heal, thereby affecting the extent and rate of drug absorption at that site. In addition, variation in skin thickness that is associated with different anatomical sites of the body has also been reported to have a direct influence on MN-based drug delivery [48]. In our study no significant differences in micropore closure time were observed between the upper arm, volar forearm, and abdomen after MN application. This result may be supported by the study of Muller *et al*, which investigated skin recovery in healthy adults after application of microarray patches to the upper arm and volar forearm by monitoring TEWL post-microarray application. They found no difference in skin recovery rates between the two sites, as TEWL response returned to baseline for both sites within 48 hr [49]. While in our current study no significant differences were observed between the anatomical sites, micropore closure time at the abdomen was overall longer than at the upper arm and volar forearm, and the number of subjects with micropore closure time exceeding 72 hr at the abdomen was more than the other two anatomical locations. While more investigation may be needed to understand the implications of these results, it is important to note that the longer micropore closure time at the abdomen may have a relationship with lower baseline skin hydration and higher skin impedance, which have been associated with longer micropore closure time [9].

In the current study we did not observe any safety concerns (local infection or intolerance) to the MNs, and historically MNs have repeatedly been shown to be safe with very low overall risk of infection. From a clinical perspective there are not likely to be major safety concerns associated with shorter or longer micropore closure times in normal, healthy individuals. Longer micropore closure times, whether a result of different intrinsic skin properties [8, 9] or application of topical treatment to prolong the micropore closure time [2, 47], have not been associated with increased risk of infection. As with any drug delivery technique that breaks the skin, it is important to properly clean the skin before applying MNs; in our study we cleaned the skin with an alcohol wipe first, which matches standard clinical protocol for injections. The MNs were also sterilized beforehand. This combined approach further reduces any safety concerns, including risk of infection. Thus the need to quantify micropore closure times is necessary not because of safety concerns, but because large differences between body sites or between patient populations would affect how much and how long a drug can be delivered through the skin. Ultimately this could have implications for ongoing efficacy of a delivered drug, making this an important point of consideration to be included in the early phases of product development.

Micropore closure half-life

Micropore closure time, described above, was determined initially by comparing admittance of MN-treated and occluded control sites in increments of 24 hr. This is not an ideal strategy in clinical settings where a more specific timeframe that accurately depicts the MN-assisted drug delivery window is highly desirable. We therefore applied a complementary strategy to estimate a more specific MN-assisted delivery window in the form of a micropore closure half-life. We have previously described the use of this method to determine micropore closure times in human subjects [9]. This predictive model can be related closely to

pharmacokinetic principles in a concept of micropore closure half-life, which then suggest a 3 – 5 half-lives timeframe at which approximately 87.5 – 97 % of micropores are expected to have closed. This micropore closure time predictive model is useful in the context of determining a window during which drug can be transdermally delivered to reach therapeutic plasma levels. The ranking of the mean micropore closure half-life in this study was abdomen \approx upper arm > volar forearm. There were no significant differences in predicted micropore closure half-lives, though our results suggest that micropores may stay open longer in the abdomen than in the upper arm and volar forearm.

Influence of skin color on measured and derived skin parameters

All of the analyses described above were performed on grouped data from all subjects, with analyses also performed on the subgroups based on subjects' self-identified racial/ethnic background. However, the use of skin color rather than racial/ethnic self-identification has been proposed as a better parameter to evaluate micropore closure time after MN application [9]. Since anatomical location and race/ethnicity both affect skin properties [11–14], we performed an additional analysis according to skin color. In this second analysis the subjects were divided into groups based on unitless L^* values of ≤ 50 ($n=10$), 51 – 65 ($n=9$), and >65 ($n=16$), rather than grouping according to self-identified race/ethnicity. Grouping according to the L^* value provides a more quantitative approach to group the subjects because of the objective nature of the colorimetry measurements (lower L^* correlates with darker skin color). For this analysis we grouped the subjects according to the measurements obtained from the abdomen because the abdomen is the least exposed to the sun on a regular basis and is likely more representative of non-tanned skin. We then compared epidermal properties and micropore closure times between the L^* groups. Figure 6 shows the distribution of L^* based skin color within the racial/ethnic groups studied.

Mean baseline TEWL at the abdomen was 4.8 ± 1.3 , 5.9 ± 1.9 , and 5.6 ± 2.0 $\text{g/m}^2 \cdot \text{hr}$ for the ≤ 50 , 51-65, and >65 groups, respectively. Although TEWL at the abdomen was lower in subjects with $L^* \leq 50$, there were no significant differences between the L^* groups. Baseline TEWL at the upper arm was 5.1 ± 1.5 , 7.4 ± 2.5 , and 6.6 ± 2.2 $\text{g/m}^2 \cdot \text{hr}$ for $L^* \leq 50$, 51-65 and >65 , respectively. Mean baseline TEWL at the volar forearm was 5.0 ± 1.9 , 6.6 ± 2.5 , and 6.2 ± 3.1 $\text{g/m}^2 \cdot \text{hr}$ for $L^* \leq 50$, 51-65, and >65 , respectively.

The mean baseline impedance at the abdomen for L^* groups ≤ 50 , 51–65, and >65 was 84.4 ± 17.8 , 79.2 ± 36.65 , and 70.0 ± 28.1 $\text{k}\Omega$, respectively. There were no statistical differences in baseline impedance when subjects were grouped by L^* but previous studies have suggested that darker skins may exhibit higher skin electrical resistance [9, 50], which correlates with trends in our current data. The mean baseline impedance at the upper arm for L^* group ≤ 50 was 72.6 ± 17.1 $\text{k}\Omega$, which was higher but not significantly different from impedance for L^* group 51-65 (58.6 ± 28.8 $\text{k}\Omega$) and >65 (65.1 ± 20.8 $\text{k}\Omega$). Mean baseline impedance at the volar forearm was 84.4 ± 21.4 , 66.4 ± 25.9 and 67.6 ± 19.5 $\text{k}\Omega$ for the ≤ 50 , 51–65, and >65 groups.

No significant difference in hydration at the abdomen was observed between L^* groups ≤ 50 (27.8 ± 6.2), 51-65 (21.4 ± 10.8), and >65 (21.4 ± 7.7). The mean baseline hydration at the upper arm for groups ≤ 50 , 51-65, and >65 was 33.2 ± 8.5 , 27.9 ± 7.8 and 24.8 ± 8.7 ,

respectively (no significant differences between groups). At the volar forearm, baseline hydration was 31.4 ± 8.5 , 28.2 ± 7.5 and 27.7 ± 8.8 for L* groups 50, 51-65, and >65, respectively.

The mean micropore closure time at the abdomen (based on statistical analysis between MN vs. control sites) was 62.4 ± 16.8 , 64.0 ± 12.0 , and 63.0 ± 12.0 hr for the 50, 51-65, and >65 groups, respectively, with no significant differences observed between groups. While mean differences in micropore closure half-life (based on the predictive model) at the abdomen were not statistically significant when subjects were grouped based on L*, mean micropore closure half-life was longer in subjects with L* 50 (28.1 ± 12.9 hr) than in subjects with L* 51-65 (20.8 ± 11.0 hr), and >65 (21.8 ± 15.3 hr). These results correlate with a previous study that showed longer micropore closure time in darker skin [9], suggesting the probable existence of a relationship between darker skin color and micropore closure half-life. This is further emphasized in the current study by the fact that a clear trend emerged when data were analyzed according to objective skin darkness/lightness, but no trend was observed when micropore closure half-lives at the anatomical sites were compared between self-identified racial/ethnic groups.

Mean micropore closure time at the upper arm for L* 50, 51-65, and >65 was 57.6 ± 16.8 , 58.7 ± 17.4 , and 63.0 ± 12.0 hr, respectively and the micropore closure half-life was 19.0 ± 12.0 , 26.2 ± 17.3 , and 24.6 ± 14.8 hr, respectively. At this anatomical location no significant differences in micropore closure time or micropore closure half-life were observed between the groups. At the volar forearm, mean micropore closure times were 64.8 ± 11.6 hr (L* 50), 56.0 ± 20.8 hr (L* 51-65) and 55.5 ± 16.9 hr (L* >65), while mean micropore closure half-life for these groups was 23.5 ± 12.3 , 19.2 ± 13.8 , and 17.4 ± 9.2 hr, respectively. These differences in micropore closure or half-life were not statistically significant. Of note, the micropore closure times and half-lives at the volar forearm followed the same trends as those at the abdomen (longer timeframes for darker skin). Table 2 shows a summary of micropore closure parameters for each anatomical site after subjects were grouped according to L*.

Importantly, when data were compared based on L* groups, no statistical difference in TEWL, impedance, hydration, micropore closure time, or micropore closure half-life was observed between the three anatomical sites. Some trends do show that the micropore resealing time is slightly longer at the abdomen and volar forearm in the darker skin types (>65). However, the observations did not follow any specific patterns at the upper arm. Because we did not see any strong trends, more investigation of these anatomical sites could be useful to fully understand if skin color is correlated with micropore closure kinetics at those sites.

Limitations

There are some limitations with this work. This was a pilot study in a small number of subjects, and that may pose a limitation on generalizing our findings. Thus, the results should be interpreted with caution. Inter-investigator differences in MN application may contribute to some variability in data collected in this study. However, we actively worked to mitigate this limitation: investigators carefully followed the same application procedures and all MN application to all anatomical sites on a subject was performed by the same

investigator. The type of MN array used in this study does not have a standard applicator, and our application approach is in line with what has been previously reported for MN arrays of this type.

Conclusion

In this pilot study we found no significant differences in barrier restoration after MN insertion at various sites on the body. This finding held true when data were grouped in three different ways: according to all subjects, self-identified race/ethnicity, and L* values. There was a trend for micropore closure time to be longer at the abdomen when compared to the upper arm and volar forearm, but further investigation would be needed to verify this. The lack of significant differences in micropore closure between anatomical sites is an encouraging finding because site of MN application may not be a notable source of variability that needs to be considered during the development of drug products.

Acknowledgments

Funding Sources

This research was supported by grant R35GM124551 from the National Institutes of Health, United States, and the American Foundation for Pharmaceutical Education Gateway to Research Award.

References

1. Prausnitz MR. Microneedles for transdermal drug delivery. *Advanced drug delivery reviews*. 2004;56(5):581–87. [PubMed: 15019747]
2. Brogden NK, Milewski M, Ghosh P, Hardi L, Crofford LJ, Stinchcomb AL. Diclofenac delays micropore closure following microneedle treatment in human subjects. *Journal of Controlled Release*. 2012;163(2):220–29. [PubMed: 22929967]
3. Jacquet E, Chambert J, Pauchot J, Sandoz P. Intra- and inter-individual variability in the mechanical properties of the human skin from in vivo measurements on 20 volunteers. *Skin Research and Technology*. 2017;23(4):491–99. [PubMed: 28370413]
4. Bodenlenz M, Augustin T, Birngruber T, Tiffner KI, Boulgaropoulos B, Schwingenschuh S, et al. Variability of Skin Pharmacokinetic Data: Insights from a Topical Bioequivalence Study Using Dermal Open Flow Microperfusion. *Pharmaceutical Research*. 2020;37(10):204. [PubMed: 32989514]
5. Lakshman KM, Bhasin S, Araujo AB. Chapter 56 - Testosterone Therapy for Osteoporosis in Men. In: Orwoll ES, Bilezikian JP, Vanderschueren D, editors. *Osteoporosis in Men (Second Edition)*. San Diego: Academic Press; 2010. p. 691–712.
6. Pastore MN, Kalia YN, Horstmann M, Roberts MS. Transdermal patches: history, development and pharmacology. *Br J Pharmacol*. 2015;172(9):2179–209. [PubMed: 25560046]
7. Donnelly RF, Singh TRR, Woolfson AD. Microneedle-based drug delivery systems: microfabrication, drug delivery, and safety. *Drug delivery*. 2010;17(4):187–207. [PubMed: 20297904]
8. Kelchen MN, Siefers KJ, Converse CC, Farley MJ, Holdren GO, Brogden NK. Micropore closure kinetics are delayed following microneedle insertion in elderly subjects. *Journal of Controlled Release*. 2016;225:294–300. [PubMed: 26829102]
9. Ogunjimi AT, Carr J, Lawson C, Ferguson N, Brogden NK. Micropore closure time is longer following microneedle application to skin of color. *Scientific Reports*. 2020;10(1):18963.
10. Brogden NK, Ghosh P, Hardi L, Crofford LJ, Stinchcomb AL. Development of in vivo impedance spectroscopy techniques for measurement of micropore formation following microneedle insertion. *J Pharm Sci*. 2013;102(6):1948–56. [PubMed: 23589356]

11. Freeman RG, Cockerell EG, Armstrong J, Knox JM. Sunlight as a factor influencing the thickness of epidermis. *Journal of Investigative Dermatology*. 1962;39(4):295–98.
12. Pinnagoda J, Tupkek R, Agner T, Serup J. Guidelines for transepidermal water loss (TEWL) measurement: a report from the Standardization Group of the European Society of Contact Dermatitis. *Contact dermatitis*. 1990;22(3):164–78. [PubMed: 2335090]
13. Schwindt DA, Wilhelm KP, Maibach HI. Water diffusion characteristics of human stratum corneum at different anatomical sites in vivo. *Journal of investigative dermatology*. 1998; 111(3):385–89.
14. Fluhr J, Dickel H, Kuss O, Weyher I, Diepgen T, Berardesca E. Impact of anatomical location on barrier recovery, surface pH and stratum corneum hydration after acute barrier disruption. *British Journal of Dermatology*. 2002;146(5):770–76.
15. Rougier A, Dupuis D, Lotte C, Roguet R, Wester R, Maibach H. Regional variation in percutaneous absorption in man: measurement by the stripping method. *Archives of dermatological research*. 1986;278(6):465–69. [PubMed: 3789805]
16. Darlenski R, Fluhr JW. Influence of skin type, race, sex, and anatomic location on epidermal barrier function. *Clinics in Dermatology*. 2012;30(3):269–73. [PubMed: 22507039]
17. Wesley NO, Maibach HI. Racial (Ethnic) Differences in Skin Properties. *American Journal of Clinical Dermatology*. 2003;4(12):843–60. [PubMed: 14640777]
18. Maibach HI, deBiologie D. Relationship between skin permeability and corneocyte size according to anatomic site, age, and sex in man. *J Soc Cosmet Chem*. 1988;39:15–26.
19. Conti A, Schiavi M, Seidenari S. Capacitance, transepidermal water loss and causal level of sebum in healthy subjects in relation to site, sex and age. *International journal of cosmetic science*. 1995;17(2):77–85. [PubMed: 19250473]
20. Machado M, Salgado TM, Hadgraft J, Lane ME. The relationship between transepidermal water loss and skin permeability. *International journal of pharmaceutics*. 2010;384(1-2):73–77. [PubMed: 19799976]
21. Mohammed D, Matts PJ, Hadgraft J, Lane ME. Variation of stratum corneum biophysical and molecular properties with anatomic site. *AAPS J*. 2012;14(4):806–12. [PubMed: 22903879]
22. Grubauer G, Elias PM, Feingold KR. Transepidermal water loss: the signal for recovery of barrier structure and function. *Journal of Lipid Research*. 1989;30(3):323–33. [PubMed: 2723540]
23. Lu F, Wang C, Zhao R, Du L, Fang Z, Guo X, et al. Review of Stratum Corneum Impedance Measurement in Non-Invasive Penetration Application. *Biosensors (Basel)*. 2018;8(2):31.
24. Emtestam L, Ollmar S. Electrical impedance index in human skin: measurements after occlusion, in 5 anatomical regions and in mi Id irritant contact dermatitis. *Contact Dermatitis*. 1993;28(2): 104–08. [PubMed: 8458202]
25. Kubisz L, Hojan-Jeziarska D, Szewczyk M, Majewska A, Kawalkiewicz W, Pankowski E, et al. In vivo electrical impedance measurement in human skin assessment. *Pure and Applied Chemistry*. 2019;91(9):1481–91.
26. Alonso A, Meirelles NC, Yushmanov VE, Tabak M. Water increases the fluidity of intercellular membranes of stratum corneum: correlation with water permeability, elastic, and electrical resistance properties. *Journal of Investigative Dermatology*. 1996;106(5).
27. Björklund S, Ruzgas T, Nowacka A, Dahi I, Topgaard D, Sparr E, et al. Skin membrane electrical impedance properties under the influence of a varying water gradient. *Biophysical journal*. 2013;104(12):2639–50. [PubMed: 23790372]
28. Morin M, Ruzgas T, Svedenhag P, Anderson CD, Ollmar S, Engblom J, et al. Skin hydration dynamics investigated by electrical impedance techniques in vivo and in vitro. *Scientific Reports*. 2020;10(1):17218. [PubMed: 33057021]
29. Verdier-Sévrain S, Bonté F. Skin hydration: a review on its molecular mechanisms. *Journal of Cosmetic Dermatology*. 2007;6(2):75–82. [PubMed: 17524122]
30. Mojumdar EH, Pham QD, Topgaard D, Sparr E. Skin hydration: interplay between molecular dynamics, structure and water uptake in the stratum corneum. *Scientific Reports*. 2017;7(1):15712. [PubMed: 29146971]

31. Suwarna UV, Deepak VM, Sheela KB, Kalpana SD. Variation in skin hydration on the basis of Deha Prakriti (body constitution): A cross-sectional observational study. *Ayu*. 2018;39(3):127. [PubMed: 31000988]
32. Logger JGM, Münchhoff CU, Olydam JI, Peppelman M, Van Erp PEJ. Anatomical site variation of water content in human skin measured by the Epsilon: A pilot study. *Skin Research and Technology*. 2019;25(3):333–38. [PubMed: 30604523]
33. Gosain A, DiPietro LA. Aging and wound healing. *World journal of surgery*. 2004;28(3):321–26. [PubMed: 14961191]
34. Greenhalgh DG. Management of the skin and soft tissue in the geriatric surgical patient. *Surgical Clinics*. 2015;95(1):103–14. [PubMed: 25459545]
35. Rawlings A, Harding C. Moisturization and skin barrier function. *Dermatologic therapy*. 2004;17:43–48. [PubMed: 14728698]
36. Sgonc R, Gruber J. Age-related aspects of cutaneous wound healing: a mini-review. *Gerontology*. 2013;59(2):159–64. [PubMed: 23108154]
37. Plensdorf S, Martinez J. Common pigmentation disorders. *American family physician*. 2009;79(2):109–16. [PubMed: 19178061]
38. Gupta J, Gill HS, Andrews SN, Prausnitz MR. Kinetics of skin resealing after insertion of microneedles in human subjects. *Journal of controlled release*. 2011;154(2):148–55. [PubMed: 21640148]
39. Bal S, Kruihof A, Liebl H, Tomerius M, Bouwstra J, Lademann J, et al. In vivo visualization of microneedle conduits in human skin using laser scanning microscopy. *Laser Physics Letters*. 2010;7(3):242–46.
40. Enfield JG, O’Connell M-L, Lawlor K, Jonathan E, O’Mahony C, Leahy MJ. In-vivo dynamic characterization of microneedle skin penetration using optical coherence tomography. *Journal of biomedical optics*. 2010;15(4):046001. [PubMed: 20799803]
41. Kochhar JS, Soon WJ, Choi J, Zou S, Kang L. Effect of microneedle geometry and supporting substrate on microneedle array penetration into skin. *J Pharm Sci*. 2013;102(11):4100–08. [PubMed: 24027112]
42. Olatunji O, Das DB, Garland MJ, Belaid L, Donnelly RF. Influence of array interspacing on the force required for successful microneedle skin penetration: theoretical and practical approaches. *J Pharm Sci*. 2013;102(4):1209–21. [PubMed: 23359221]
43. Gill HS, Denson DD, Burris BA, Prausnitz MR. Effect of microneedle design on pain in human subjects. *The Clinical journal of pain*. 2008;24(7):585. [PubMed: 18716497]
44. Kalluri H, Kolli CS, Banga AK. Characterization of microchannels created by metal microneedles: formation and closure. *AAPS J*. 2011;13(3):473–81. [PubMed: 21732220]
45. Qiu Y, Gao Y, Hu K, Li F. Enhancement of skin permeation of docetaxel: a novel approach combining microneedle and elastic liposomes. *Journal of Controlled Release*. 2008;129(2):144–50. [PubMed: 18538885]
46. Wermeling DP, Banks SL, Hudson DA, Gill HS, Gupta J, Prausnitz MR, et al. Microneedles permit transdermal delivery of a skin-impermeant medication to humans. *Proceedings of the National Academy of Sciences*. 2008;105(6):2058–63.
47. Brogden NK, Banks SL, Crofford LJ, Stinchcomb AL. Diclofenac enables unprecedented week-long microneedle-enhanced delivery of a skin impermeable medication in humans. *Pharmaceutical research*. 2013;30(8):1947–55. [PubMed: 23761054]
48. Larraneta E, Lutton RE, Woolfson AD, Donnelly RF. Microneedle arrays as transdermal and intradermal drug delivery systems: Materials science, manufacture and commercial development. *Materials Science and Engineering: R: Reports*. 2016;104:1–32.
49. Muller DA, Henricson J, Baker SB, Togö T, Jayashi Flores CM, Lemaire PA, et al. Innate local response and tissue recovery following application of high density microarray patches to human skin. *Scientific Reports*. 2020;10(1):18468. [PubMed: 33116241]
50. Johnson LC, Corah NL. Racial differences in skin resistance. *Science*. 1963;139(3556):766–67. [PubMed: 17829126]

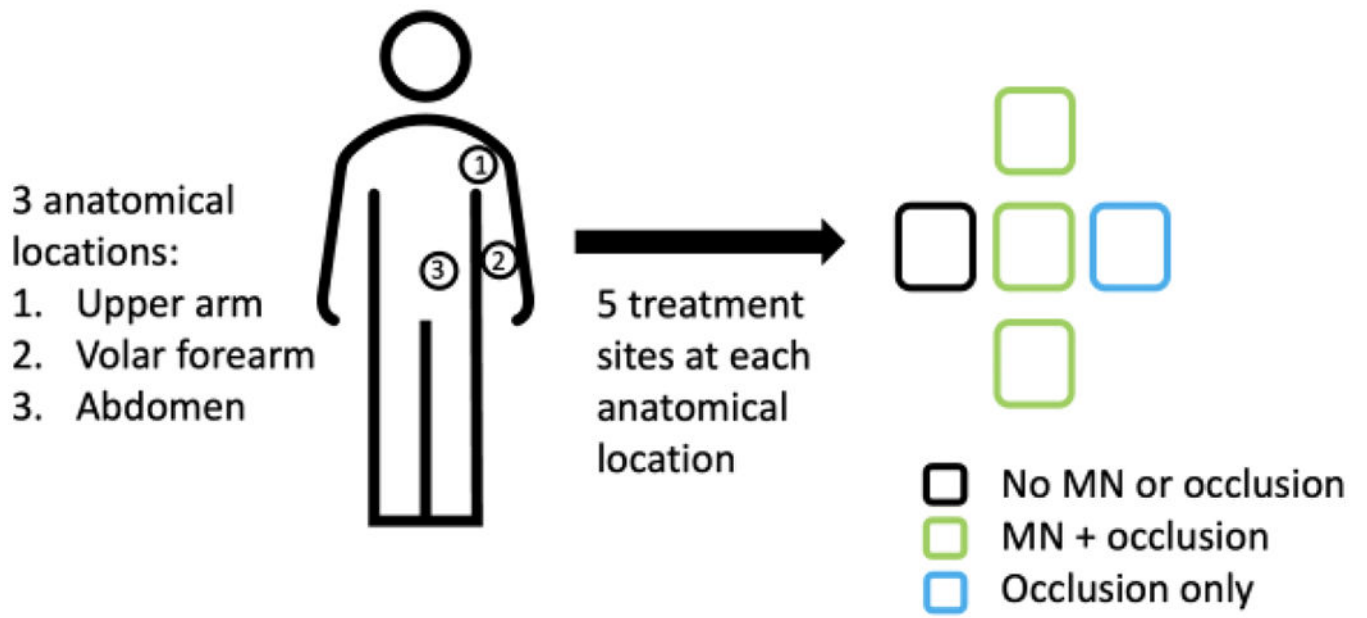


Figure 1. Three anatomical locations were studied: upper arm, volar forearm, and abdomen. Five treatment sites were identified at each of the 3 anatomical locations.

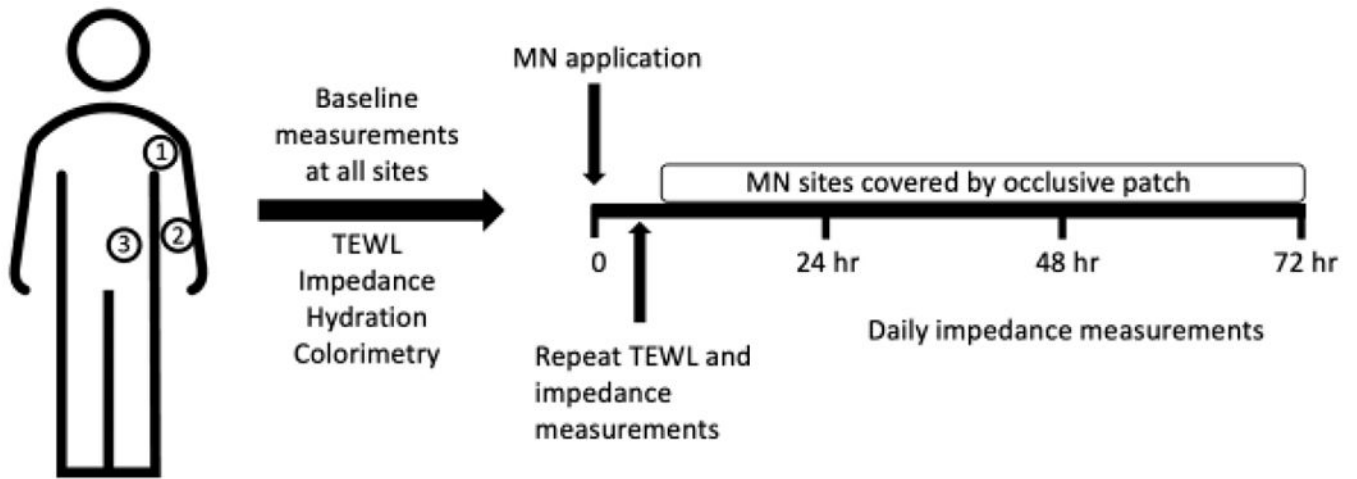


Figure 2.

Visual representation of overall clinical study design for the sites treated with MNs. The same study design and timeline was used for all treatment sites at each anatomical location, but the unoccluded control sites did not receive MN treatment (the sites were covered with an occlusive patch for the same duration), and the other control sites did not receive MN treatment or occlusion.

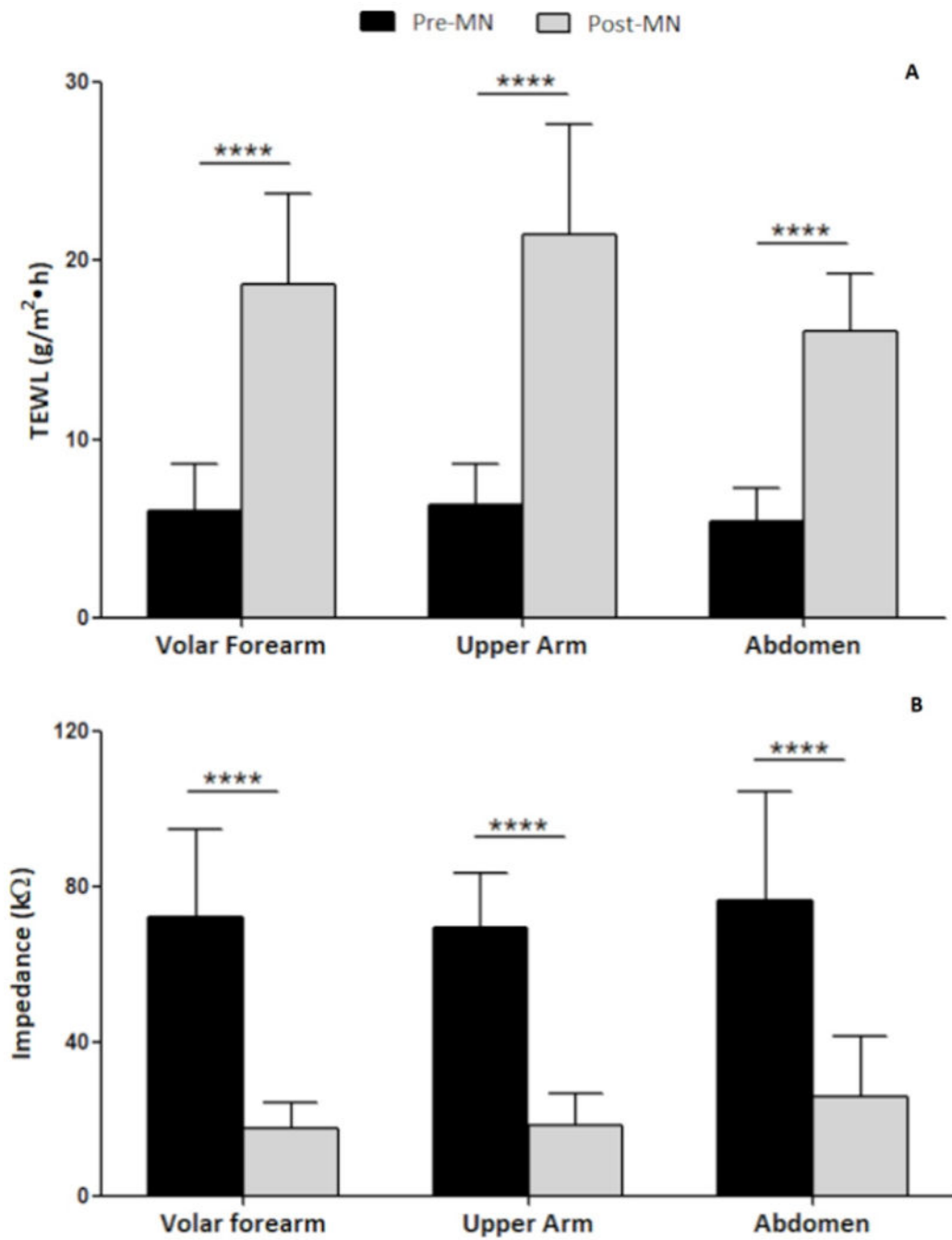


Figure 3: Pre- and post-MN (A) TEWL and (B) impedance at the three anatomical locations. Data presented as mean \pm SD of all subjects (n=35). **** $p < 0.0001$

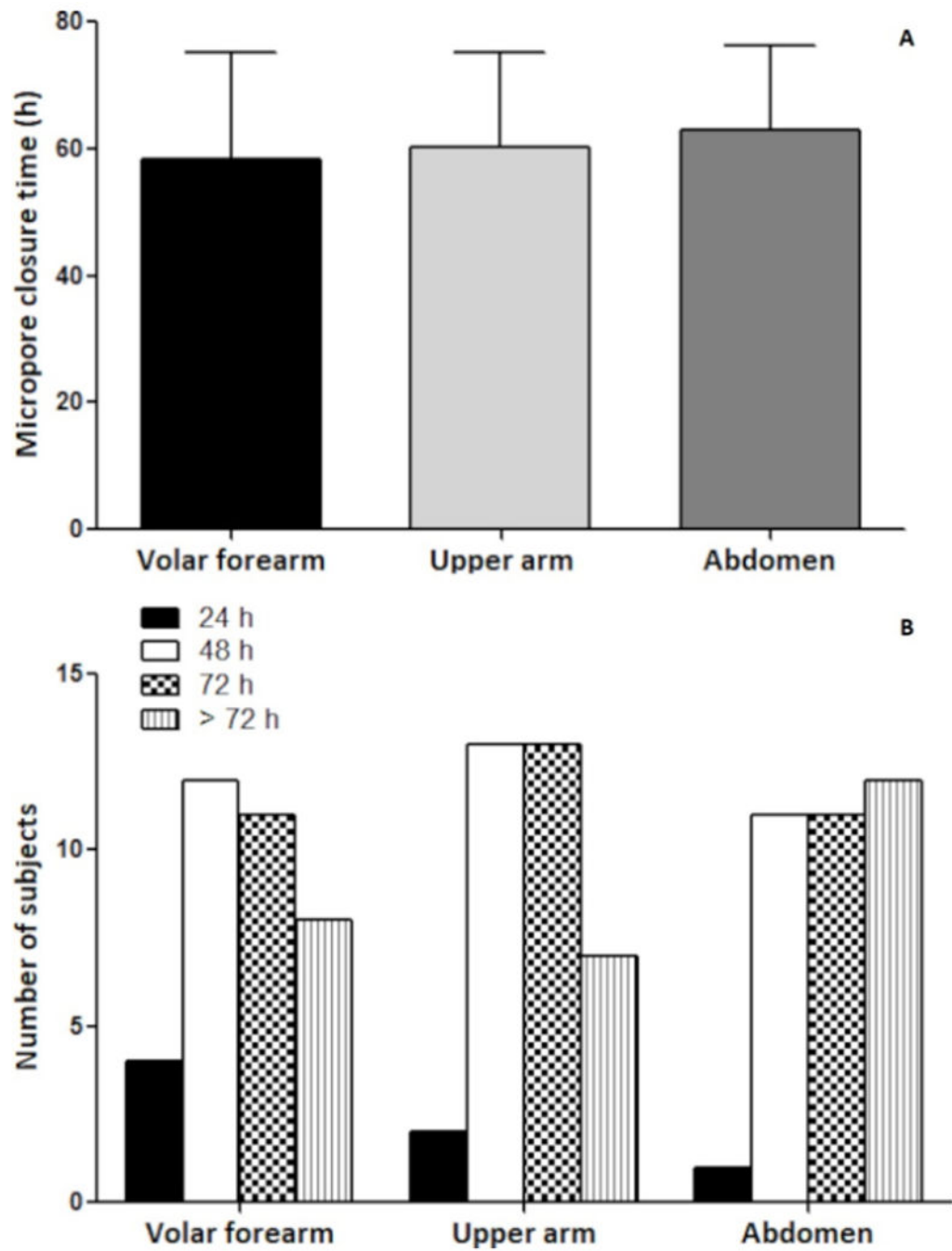


Figure 4: Graph showing (A) mean and (B) frequency distribution of micropore closure time at each anatomical location. Data presented as mean \pm SD of all subjects (n=35).

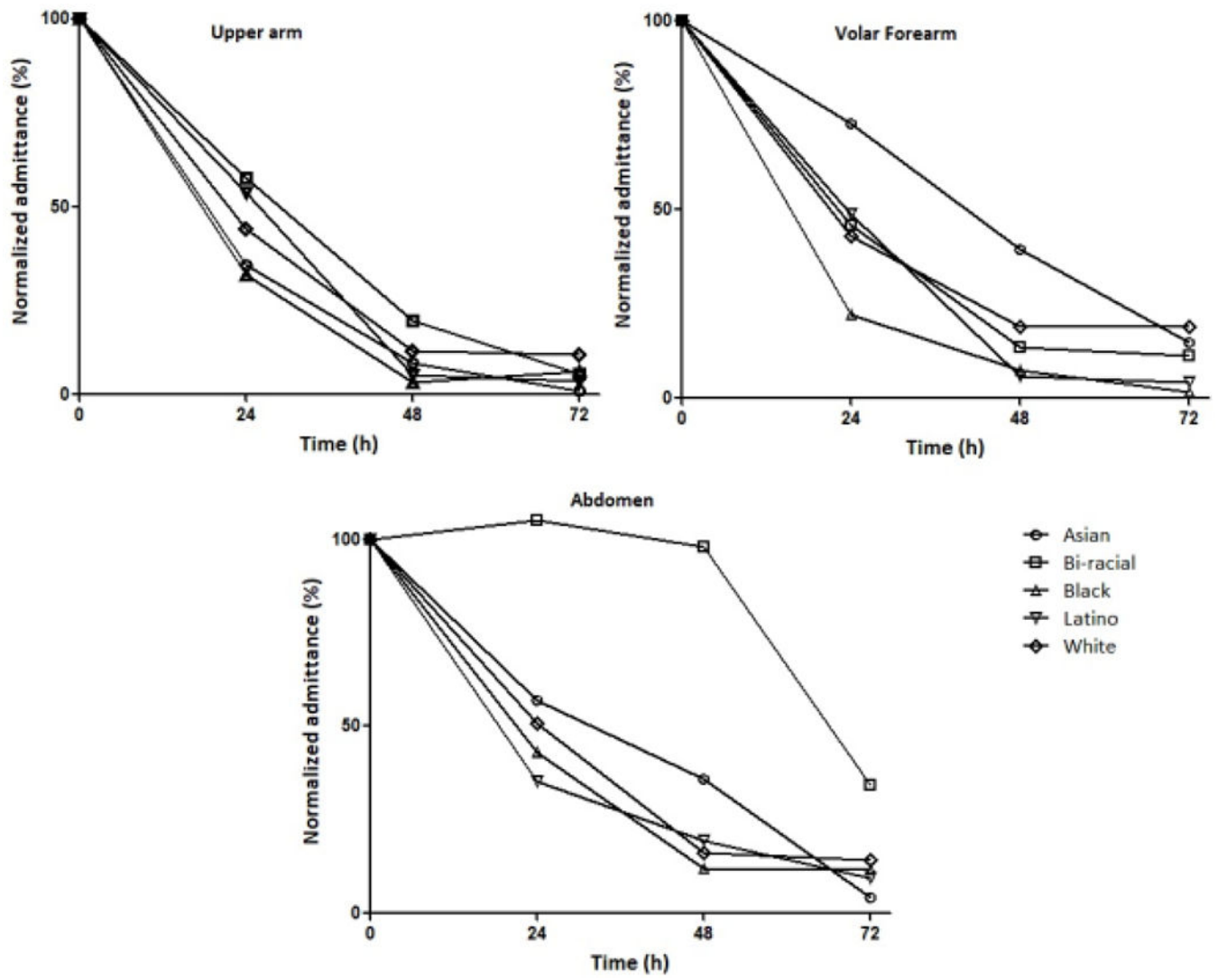


Figure 5: Normalized micropore admittance vs. time plots. Each line represents one representative subject from each group.

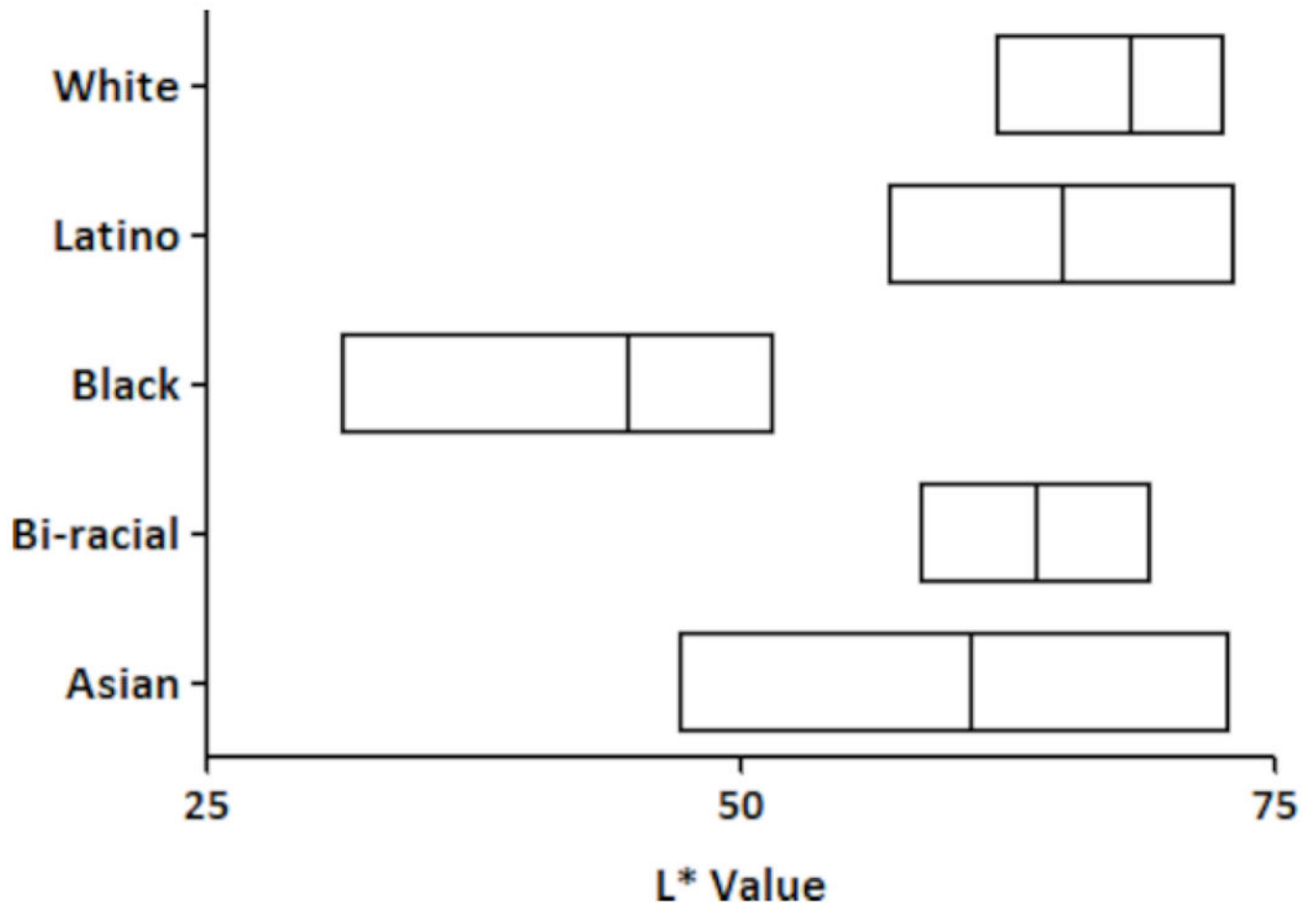


Figure 6: L* skin color distribution among participants from self-identified racial/ethnic groups. The measurements from the abdomen site were used for the L* value. Boxes represent the range of values, and the line within each box represents the mean L*.

Table 1:

Summary of baseline and post-MN epidermal properties. Subjects are groups according to self-identified race/ethnicity. Skin hydration and L* are unitless measurements.

Racial group	Anatomical site	Baseline TEWL (g/m ² •hr)	TEWL % increase post-MN	Baseline impedance (k Ω)	Impedance % decrease post-MN	Baseline skin hydration	Baseline L* value
Asian	Upper Arm	6.92 \pm 1.52	250.72 \pm 66.66	64.50 \pm 21.12	70.60 \pm 13.02	23.90 \pm 6.42	59.40 \pm 9.46
	Volar forearm	7.68 \pm 4.01	218.78 \pm 73.63	67.33 \pm 25.11	75.89 \pm 8.21	24.36 \pm 4.36	60.50 \pm 7.68
	Abdomen	5.68 \pm 1.83	225.50 \pm 77.18	86.90 \pm 32.30	62.87 \pm 14.65	18.59 \pm 5.95	60.85 \pm 9.99
Bi-/multi-racial	Upper Arm	5.69 \pm 0.86	195.05 \pm 5.30	57.55 \pm 3.89	76.15 \pm 6.01	35.47 \pm 12.35	58.86 \pm 9.19
	Volar forearm	5.73 \pm 0.59	179.85 \pm 22.84	58.00 \pm 5.37	73.90 \pm 2.97	30.19 \pm 10.82	62.50 \pm 5.63
	Abdomen	5.18 \pm 0.21	193.45 \pm 9.97	49.95 \pm 5.87	64.20 \pm 15.41	37.24 \pm 13.18	63.86 \pm 7.64
Black	Upper Arm	4.53 \pm 1.53	302.99 \pm 118.57	78.78 \pm 16.41	77.80 \pm 9.06	35.08 \pm 7.75	46.69 \pm 8.56
	Volar forearm	4.69 \pm 1.97	315.31 \pm 126.22	85.86 \pm 19.99	78.63 \pm 4.74	32.46 \pm 8.73	50.82 \pm 7.20
	Abdomen	4.87 \pm 1.40	214.29 \pm 89.62	81.51 \pm 15.53	74.20 \pm 6.51	27.98 \pm 5.92	44.72 \pm 6.78
Latino	Upper Arm	7.56 \pm 2.64	203.42 \pm 34.03	58.87 \pm 28.83	57.90 \pm 18.50	24.12 \pm 4.39	62.80 \pm 5.76
	Volar Arm	6.15 \pm 2.25	225.40 \pm 77.69	68.65 \pm 24.72	68.57 \pm 8.97	28.76 \pm 8.59	63.80 \pm 5.04
	Abdomen	5.77 \pm 2.38	195.43 \pm 56.89	83.55 \pm 36.35	58.18 \pm 16.17	18.03 \pm 5.51	65.07 \pm 6.00
White	Upper Arm	6.98 \pm 2.67	236.21 \pm 91.47	78.48 \pm 16.41	77.80 \pm 9.06	26.02 \pm 10.12	64.98 \pm 2.19
	Volar forearm	5.50 \pm 1.34	252.63 \pm 91.75	68.58 \pm 20.90	72.89 \pm 5.92	29.60 \pm 9.90	67.38 \pm 1.95
	Abdomen	5.64 \pm 2.16	282.30 \pm 142.41	62.20 \pm 25.02	64.04 \pm 9.87	23.52 \pm 8.77	68.22 \pm 3.17

Table 2:

Micropore closure kinetics when subjects were grouped according to the following L* values: 50 (n=10), 51 – 65 (n=9), and >65 (n=16).

L* group	Micropore closure time, hr			Micropore closure $t_{1/2}$, hr			3-5 half-lives, hr		
	50	51 – 65	>65	50	51 – 65	>65	50	51 – 65	>65
Upper arm	57.6 ± 16.8	58.7 ± 17.4	63.0 ± 12.0	19.0 ± 12.0	26.2 ± 17.3	24.6 ± 14.8	57.1 – 95.2	78.6 – 131.1	73.8 – 123.0
Volar forearm	64.8 ± 11.6	56.0 ± 20.8	55.5 ± 16.9	23.5 ± 12.3	19.2 ± 13.8	17.4 ± 9.2	70.5 – 117.5	57.6 – 96.0	52.2 – 87.0
Abdomen	62.4 ± 16.8	64.0 ± 12.0	63.0 ± 12.0	28.1 ± 12.9	20.8 ± 11.0	21.8 ± 15.3	84.3 – 140.5	62.4 – 104.0	65.4 – 109.0